Waste Management 67 (2017) 181–192

Contents lists available at ScienceDirect

Waste Management

journal homepage: www.elsevier.com/locate/wasman

A two-stage treatment for Municipal Solid Waste Incineration (MSWI) bottom ash to remove agglomerated fine particles and leachable contaminants

Qadeer Alam *, M.V.A. Florea, K. Schollbach, H.J.H. Brouwers

Department of the Built Environment, Eindhoven University of Technology, P.O. Box 513, 5600 MB Eindhoven, The Netherlands

ARTICLE INFO

Article history:
Received 20 October 2016
Revised 15 May 2017
Accepted 16 May 2017
Available online 1 June 2017

Keywords:
MSWI bottom ash
Potentially toxic elements
Chloride leaching
Washing

ABSTRACT

In this lab study, a two-stage treatment was investigated to achieve the valorization of a municipal solid waste incineration (MSWI) bottom ash fraction below 4 mm. This fraction of MSWI bottom ash (BA) is the most contaminated one, containing potentially toxic elements (Cu, Cr, Mo and Sb), chlorides and sulfates. The BA was treated for recycling by separating agglomerated fine particles (≤125 μm) and soluble contaminants by using a sequence of sieving and washing. Initially, dry sieving was performed to obtain BA-S (≤125 μm), BA-M (0.125–1 mm) and BA-L (1–4 mm) fractions from the original sample. The complete separation of fine particles cannot be achieved by conventional sieving, because they are bound in a cementitious matrix around larger BA grains. Subsequently, a washing treatment was performed to enhance the liberation of the agglomerated fine particles from the BA-M and BA-L fractions. These fine particles were found to be similar to the particles of BA-S fraction in term of chemical composition. Furthermore, the leaching behavior of Cr, Mo Sb, chlorides and sulfates was investigated using various washing parameters. The proposed treatment for the separation of agglomerated fine particles with dry sieving and washing (L/S 3, 60 min) was successful in bringing the leaching of contaminants under the legal limit established by the Dutch environmental norms.

1. Introduction

In The Netherlands, municipal solid waste incineration (MSWI) is extensively used as an efficient waste management system for non-recyclable waste materials (Hjelmar, 1996). However, incineration produces large quantities of by-products, among which bottom ash (BA) is the most abundant with respect to the generated volumes (Margallo et al., 2015). In order to move towards a circular economy, the utilization of BA in building materials as a secondary raw material is preferred over landfilling. Furthermore, stringent state regulations, land scarcity and high taxation on landfilling have generated increased interest in research initiatives to maximize the recycling potential of BA (Dutch Ministry of Infrastructure and Environment, 2012; Soil Quality Decree, 2013).

After incineration, BA undergoes further treatments such as separation of unburnt materials, removal of ferrous and non-ferrous metals, sieving and washing to produce a recyclable fraction. After treatment, a size-fractionated BA (4–32 mm) is usually recycled as loose aggregate in concrete (Juric et al., 2006), road construction (Hjelmar et al., 2007) and acoustic barriers (Pera et al., 1997). In addition to recyclable BA, this process also yields a residual fraction of BA, which is considered rich in contaminants (Chimenos et al., 2000, 2003). Its application is limited, beyond a potential for recovering valuable metals (Tang and Steenari, 2015). Furthermore, many researchers have studied the particle size dependency of the potentially toxic elements (PTEs) in the incinerated by-products (Alba et al., 1997; Chandler et al., 1997; Florea and Brouwers, 2015; Tang et al., 2015; Wang et al., 2002). It is reported that the content of chlorides in the MSWI bottom ash strongly increases with the size of its particles (Alam et al., 2016; Yang et al., 2014). Consequently, due to their high content of leachable contaminants such as chlorides, sulfates and PTEs (As, Cu, Cr, Cd, Co, Hg, Mo, Ni, Pb and Sb), this fraction can only be used in restricted applications such as liner and covers. These applications require extensive monitoring and care in order to limit the environmental damage from theses pollutants. Due to the recent Dutch initiative "Green Deal B-76" the utilization of BA in the aforementioned applications will not be a viable option starting in 2020 (Dutch Ministry of Infrastructure and Environment, 2012). This implies that treatment methods need

* Corresponding author.
E-mail address: q.alam@tue.nl (Q. Alam).

http://dx.doi.org/10.1016/j.wasman.2017.05.029
0956-053X/

to be developed for the use of this fraction in different applications as well.

The washing of size-separated fractions of incineration by-products is extensively investigated in order to extract soluble contaminants (Boghetich et al., 2005; Chimenos et al., 2005; Doudart de la Grée et al., 2016; Ito et al., 2008; Keulen et al., 2012; Kim et al., 2005; Wang et al., 2016; Yang et al., 2012). Particularly, in the Netherlands, washing treatments are currently being applied for the recycling of BA. However, the liberation of agglomerated fine particles from the surface of coarser particles during the size-separation and washing treatment is often over-looked. It is reported that these fine particles mainly contain quenching and weathering products (Eighmy et al., 1994; Eusden et al., 1999), primarily because of their high surface area. These quenching products are formed when BA is cooled down by discharging in water after the incineration. During the quenching process numerous reactions (dissolution, oxidation, hydration and carbonation) start taking place at the particle surface, which result in binding and agglomeration of fine particles in the C-S-H gel on the surface of BA (Inkaew et al., 2016). Due to the agglomeration and moisture content of BA, conventional sieving is limited in achieving complete removal of these fine particles. Tang et al. (2016) reported their removal from the surface of MSWI bottom ash by applying slow milling in combination with thermal treatment, which led to a decrease in the leachability of contaminants. However, the removal of agglomerated fine particles without other treatments was insufficient in reducing the contaminants below the permissible limits.

In this lab-scale study, the particle size dependency of contaminants was utilized to produce clean fractions of BA. Therefore, the initial BA (≤4 mm) was separated by dry sieving into three different fractions, BA-S (≤0.125 mm), BA-M (0.125–1 mm) and BA-L (1–4 mm). Then, a two-stage treatment based on sieving and washing was investigated to maximize the removal of agglomerated fine particles and soluble contaminants from bigger fractions of BA in order to fulfill the requirements established by the Soil Quality Decree (2013). Furthermore, the leaching behavior of contaminants under the influence of various washing parameters (liquid-to-solid ratio, washing duration) was investigated.

2. Materials and methods

2.1. Materials

BA ≤ 4 mm used in this study was provided by Heros Sluiskil, the Netherlands. This fraction was produced by applying a number of standard dry pre-treatments, such as screening, removal of unburnt material, separation of ferrous and non-ferrous metals and sorting the complete range of BA (Holm and Simon, 2017). Before applying these treatments, the BA from incineration was weathered for 6 weeks. Other incineration residues, such as fly ash and flue gas residue, were not added to the BA after the incineration process.

2.2. Methods

2.2.1. Chemical and physical analysis of solids

Original BA, as received, was sieved into three different fractions using a vibratory sieve shaker (Restch; AS 450 Basic) with mesh sizes of 125 μm, 1 mm and 4 mm (DIN EN 933-2) to separate the BA-S (≤0.125 mm), BA-M (0.125–1 mm) and BA-L (1–4 mm) fractions, respectively. The sieving was performed according to the DIN EN 933-1. The particle size distribution of fractions containing particles ≤ 0.125 mm was determined using laser diffraction (Mastersizer 2000 Malvern) in the presence of sonication to disperse the particles.

For chemical and mineralogical analysis, these fractions were milled in a planetary ball mill (Fritsch; Pulverisette 5) for 20 min at 120 rpm. Afterwards, a semi-quantitative chemical analysis of the all BA fractions was carried out by measuring pressed powder with an X-ray fluorescence spectrometer (XRF; PANalytical Epsilon 3). The data was analyzed with the Omnian method (standardless). To determine chlorine content in the initial fractions of BA accurately, quantification was performed by using Instrumental Neutron Activation Analysis (INAA). A computerized-rabbit-system was used for the irradiation of samples at the thermal flux of 7×10^{12} n cm^{-2} s^{-1}. The chlorine content in the samples was measured after allowing appropriate time for the decay of short lived isotopes. Furthermore, the identification of the crystalline phases in the bulk sample was performed with an X-ray diffractometer (XRD; Siemens D5000) with Cu Kα radiation, a step size of 0.02° and a monochromator. The XRD diffractograms were analyzed with X'pert high score plus software from PANalytical. The loss on ignition (LOI) for the BA fractions was measured at 1000 °C until a constant mass was obtained according to EN ISO 3262-1.

The morphology and internal structure of the un-sieved BA (≤4 mm) was investigated by analyzing a cross-section of sample with scanning electron microscopy (SEM; JEOL JSM-7001) in a backscattered electron (BSE) mode. Furthermore, elemental mapping was performed by using energy dispersive X-ray spectroscopy (EDS). The samples for this measurement were cast in resin without using water for the preparation.

2.2.2. Generation and analysis of leachates

In order to investigate the separation of agglomerated fine particles and contaminants, the BA-M or BA-L fraction and distilled water were mixed in polyethylene bottles to obtain different liquid-to-solid (L/S) (L kg^{-1}) ratios. Afterwards, these bottles were sealed and placed horizontally on a linear reciprocating shaking device (Stuart SSL2) for washing at a constant rate of 250 rpm with the amplitude of 20 mm. The washing experiments were performed at room temperature for the duration of 3 min, 60 min and 72 h. After the extraction, leachates were filtered and acidified using 0.2% (vol.%) of 15 M ultrapure HNO_3. The PTEs content in the leachates was determined by inductively coupled plasma-optical emission spectroscopy (ICP-OES; Varian 730-ES). A potentiometric titration was performed with an ion specific electrode (Ag/AgCl) to measure the concentration of chlorides in the leachates. These measurements were performed in triplicate with a Metrohm 785 DMP Titrino. Furthermore, the concentration of sulfates (SO_4^{2-}) was analyzed by an ion chromatograph (Dionex 1100) equipped with ion exchange column AS9-HS (2 × 250 mm). A 9 mM solution of Na_2CO_3 was used as an eluent with an isocratic flow of 0.25 ml min^{-1}. The detection of ions was done by measuring suppressed conductivity using an electrolytically regenerated suppressor (Dionex AERS 500, 2 mm). The content of contaminants was corrected to the dry matter (DM) of BA and reported in mg/kg.

2.2.3. Treatment methodology

A two-stage treatment, washing (with distilled water) and separation of the agglomerated fine particles (≤125 μm) was designed and investigated for treating the BA. An overview of the treatment for the MSWI bottom ash is provided in Fig. 1. The leachability of the BA-S, BA-M and BA-L fractions was assessed by applying a preliminary washing treatment at L/S 12 for 72 h (Section 3.1.2.). These washing parameters were found to be more efficient in extracting contaminants as compared to the column leaching test performed according to NEN-EN 12457-4 (Alam et al., 2016). On the basis of these results, the BA-S fraction was separated and no treatment was performed due to its initial high content of contaminants. Afterwards, the BA-M and BA-L fractions were washed at

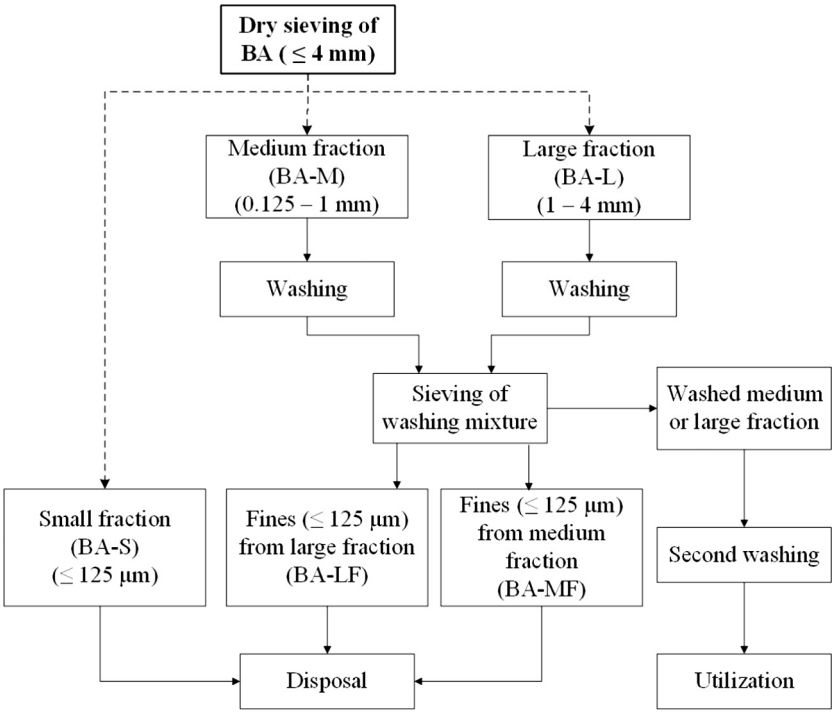

Fig. 1. Schematic representation of the two-stage washing treatment applied to the MSWI bottom ash for the separation of fine particles and contaminants.

different L/S ratios and the washing mixtures were sieved to further enhance the separation of the fine particles (≤125 μm). These fine particles liberated from the BA-M and BA-L fractions will be referred to as BA-MF and BA-LF, respectively. After the liberation of these fine particles, a second washing cycle was performed on BA-M and BA-L to bring the leaching of contaminants under the legal limit.

3. Result and discussion

3.1. Characterization of BA fractions

The size distribution of the bulk BA in different fractions is presented in Fig. 2a. The BA-M and BA-L fractions comprise more than 90% (m/m) of the un-sieved BA. The rest of BA was distributed between the BA-S fraction and particles with diameter >4 mm. The latter fraction was not investigated further in the study.

3.1.1. Mineralogical and chemical analysis

In Fig. 3 the XRD diffractograms of all three fractions of BA are provided. The main crystalline components are quartz (SiO_2) and calcite ($CaCO_3$). Calcite tends to accumulate in the BA-S fraction, while quartz shows the inverse trend and is concentrated in fractions containing bigger particles (BA-M and BA-L). This trend is in accordance with the elemental content of Ca and Si of these fractions, provided in Table 1. Other phases visible in all three fractions and their general formula are as follows: spinel in the form of magnetite (Fe_3O_4), microcline ($KAlSi_3O_8$), melilite $(Ca,Na)_2(Al,Mg,Fe^{2+})$

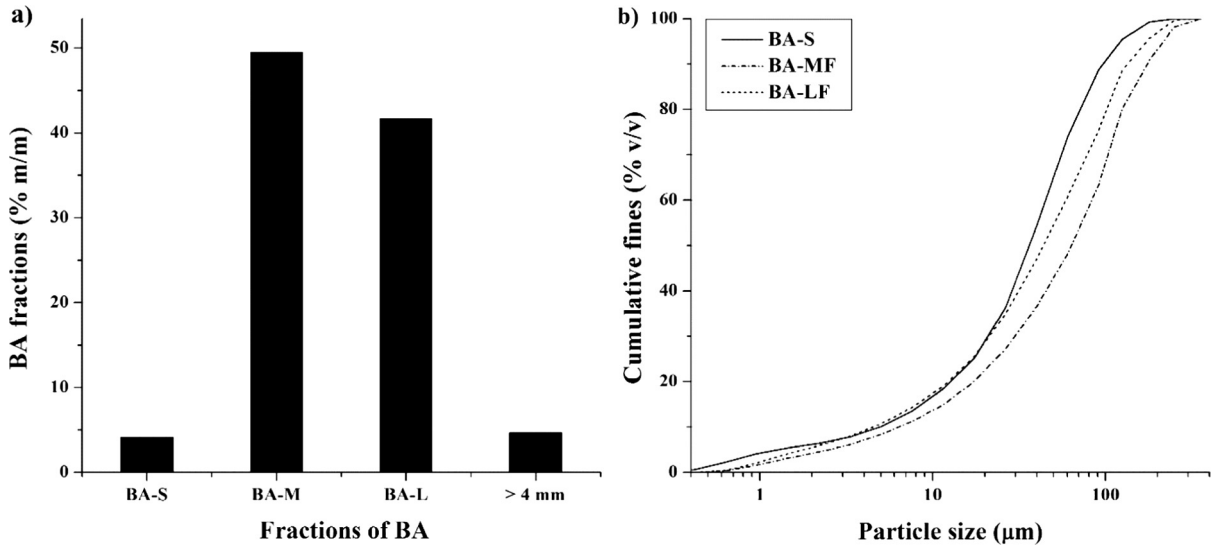

Fig. 2. Distribution of the initial BA into different particle size ranges. (a) Mass % of the BA-S (≤125 μm), BA-M (0.125–1 mm), and BA-L (1–4 mm) fractions. (b) Particle size distribution of the BA-S, BA-MF and BA-LF fractions.

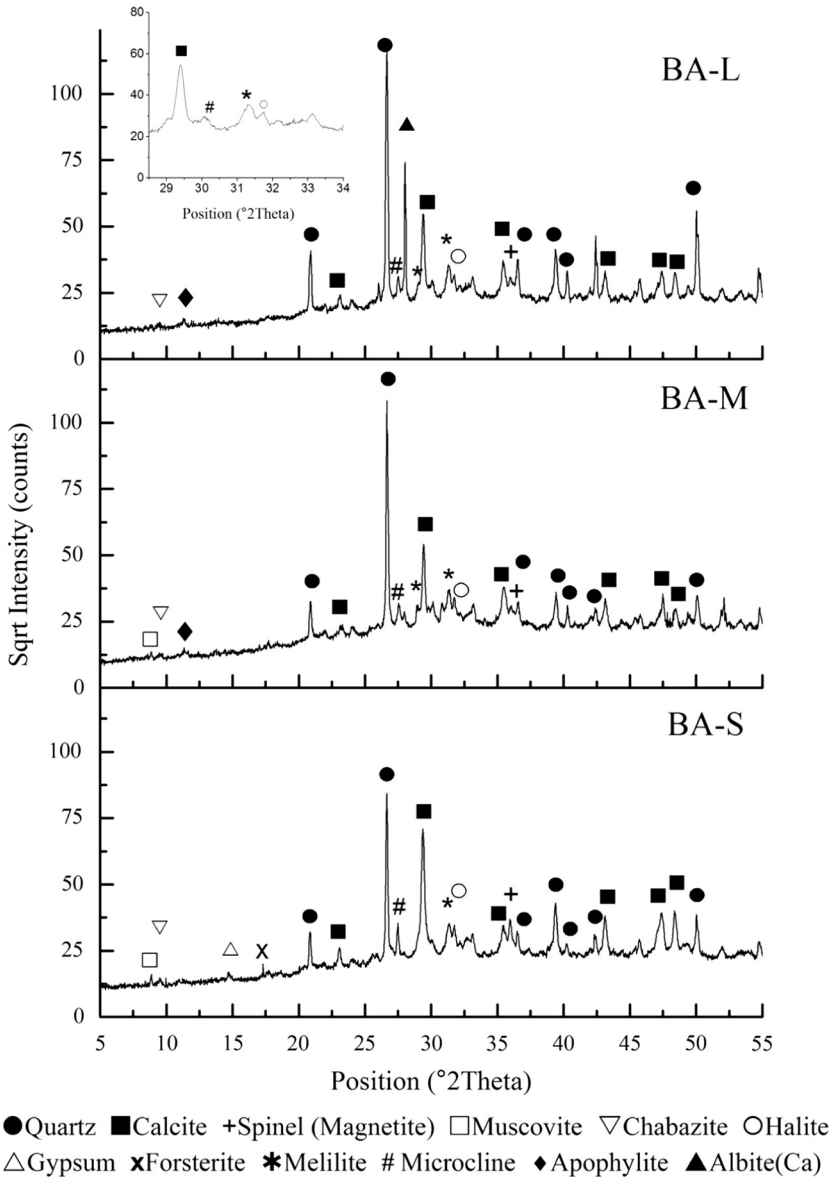

Fig. 3. Crystalline phases in BA-S (≤125 μm), BA-M (0.125–1 mm), and BA-L (1–4 mm) fractions of MSWI bottom ash.

Table 1
Elemental composition (% m/m) of the all three BA fractions in elemental form measured by XRF. R.E. (Remaining elements) and loss on ignition at 1000 °C ($LOI_{1000\,°C}$).

	Ca	Si	Fe	Al	S	P	Mg	Na	Ti	Cl	K	R.E.	LOI	Cl*
BA-S	34.4	7.9	8.5	7.7	2.7	1.0	1.1	1.2	1.6	2.1	1.3	3.1	27.5	1.2
BA-M	28.6	13.2	13.4	6.9	2.5	1.1	1.2	1.3	1.5	1.8	1.4	2.9	24.2	0.9
BA-L	27.6	15.6	17.7	6.6	2.1	1.2	1.7	1.8	1.4	1.6	1.6	2.7	18.5	0.7

* Quantitatively determined with INAA.

$(Al,Si)SiO_7$, the zeolite; chabazite $(Ca,Na_2,K_2,Mg)Al_2Si_4O_{12}{\cdot}6H_2O$ and halite (NaCl). Moreover, low amounts of gypsum ($CaSO_4{\cdot}2H_2O$) are visible only in the small fraction. Other minerals identified are forsterite (Mg_2SiO_4), apophylite $(K,Na)Ca_4Si_8O_{20}(F,OH){\cdot}8H_2O$ and Ca-rich albite $(Na,Ca)Al(Si,Al)_3O_8$.

The chemical composition of the BA fractions (after accounting for LOI) in term of major and minor elements (% m/m) obtained by XRF is provided in Table 1. The distribution of major elements, Ca, Si, and Fe varies with the BA particle size. The content of Ca and Cl increases with the decrease in the particle size of the BA fractions, while the inverse holds true for the Si and Fe content.

3.1.2. Leachability of contaminants from BA fractions

The emission of PTEs, halides and sulfates from the initial BA (≤4 mm) and its size-separated fractions along with their regulatory limit (Soil Quality Decree, 2013) is provided in Table 2. In original BA and all three size-separated fractions, the contents of Cr, Cu, Mo, Sb, Cl^- and SO_4^{2-} exceeded the emission limit specified for use in unrestricted applications. In addition to that, trace quantities of As, Ni, Pb, Cd, and Zn were also found in the washing leachates. However, the contents of these trace metals were well below their legal emission limit.

Table 2
Leachable content of PTEs, halides and sulfates from the original BA (≤4 mm), BA-S (≤125 μm), BA-M (0.125–1 mm), and BA-L (1–4 mm) fractions and their allowed emission limits regulated by the Soil Quality Decree (2013).

Parameters	Non-shaped materials[a] [mg/kg$_{DM}$]	≤4 mm BA[b] [mg/kg$_{DM}$]	BA-S[c] [mg/kg$_{DM}$]	BA-M[c] [mg/kg$_{DM}$]	BA-L[c] [mg/kg$_{DM}$]
Ba	22	0.69	0.821	0.663	0.724
Cr	0.63	0.12	1.786	0.651	0.414
Cu	0.9	14	9.643	2.558	1.954
Mo	1	1.1	2.024	1.023	1.011
Sb	0.32	0.22	0.821	0.663	0.724
As	0.9	<0.05	0.060	0.058	0.057
Cd	0.04	<0.001	<L.D.	<L.D.	<L.D.
Co	0.54	<0.030	0.036	0.035	0.034
Pb	2.3	<0.1	0.119	0.116	0.115
Ni	0.44	0.24	0.077	0.058	0.057
Se	0.15	<0.007	<L.D.	<L.D.	<L.D.
Sn	0.4	<0.02	<L.D.	<L.D.	<L.D.
V	1.8	<0.1	<L.D.	<L.D.	<L.D.
Zn	4.5	0.48	<L.D.	<L.D.	<L.D.
Cl^-	616	6200	11013	7516	6354
Br^-	20	–	21.4	11.4	9.3
F^-	55	2.4	6.5	3.9	3.2
SO_4^{2-}	1730	1700	9404	2558	3120
pH	–	11.28	9.57	10.92	10.86

<L.D. – Concentration of the element was below the detection limit.
DM – Dry Matter.
[a] Leaching limit imposed by the Soil Quality Decree (2013) for non-shaped building materials.
[b] Column leaching test was performed in accordance with NEN-EN 12457-4.
[c] Content of the elements in the leachates extracted by washing with L/S 12 for 72 h.

In Fig. 4, a comparison between the leaching of contaminants (Cr, Cu, Mo, Sb, Cl^- and SO_4^{2-}) from BA-S, BA-M and BA-L fractions is provided. The leaching of these contaminants was found to be well above their legal regulatory limit. The leachable content of Cu and Cr demonstrates clear dependence on the particle size of the BA fractions (Fig. 4a). The content of these metals in the BA fractions was inversely proportional to the particle size. In the case of Cu, a substantial change in distribution across different fractions was observed: more than 70% of the total leachable Cu content was generated by the BA-S fraction. Furthermore, higher contents of Mo and Sb were also noted in this fraction as compared to the BA-M and BA-L fractions. While the bigger fractions of BA have a similar contents of leachable Mo and Sb. On the other hand, the leachable content of chlorides and sulfates (Fig. 4b) were also concentrated in the BA-S fraction. The contents of chlorides show a gradual decrease when the particle size of BA fractions increases. Especially, the leachable contents of Cr, Cu, Mo, Cl^- and SO_4^{2-} have a tendency to accumulate in particles with a sizes ≤ 125 μm.

The high content of contaminants in the BA-S fraction can be explained by the quenching process of BA. Water quenching is the most widely used treatment for the cooling of incineration residue in waste-to-energy plants (Bourtsalas, 2013). Furthermore, a high concentrations of the soluble salts in the quenching water (because of its frequent re-use) facilitates the co-precipitation of chemical species on the surface of the BA. During this process, dissolution, carbonation, oxidation and hydration reactions occur on the surface of the particles (Inkaew et al., 2016). Subsequently, it leads to the co-precipitation and adsorption of PTEs and chlorides from the quenching water into newly formed phases such as gypsum, ettringite, hydrocalumite and portlandite, (Bayuseno and Schmahl, 2010; Ito et al., 2008; Speiser et al., 2000). Since, the residence time of BA in the quenching water is short, most of the reac-

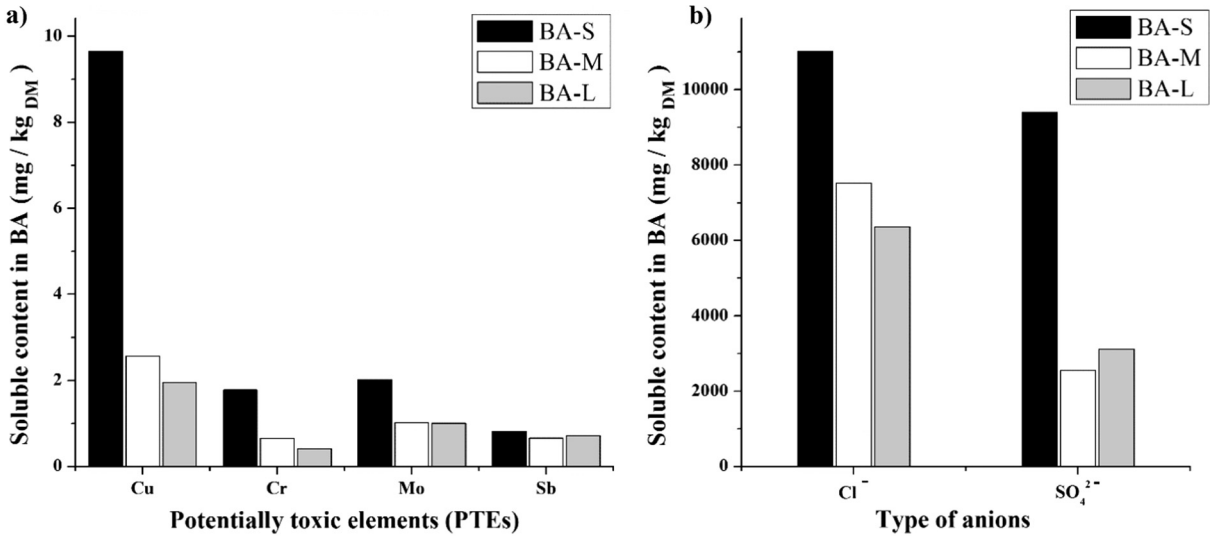

Fig. 4. Soluble content of contaminants in different fractions of BA. (a) The contents of Cu, Cr, Mo and Sb across different fractions of BA. (b) The contents of chlorides and sulfates (determined by washing with L/S 12 for the duration of 72 h).

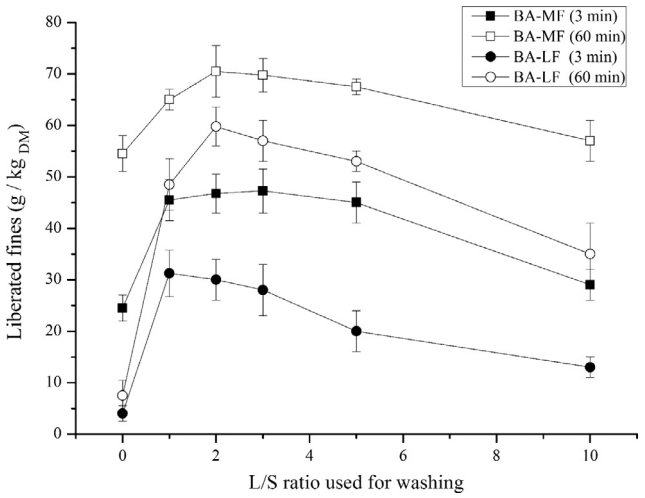

Fig. 5. Influence of the washing time (3 and 60 min) and the L/S ratio on the separation of fines (designated as BA-MF and BA-LF for the fines separated from the BA-M and BA-L fractions, respectively). L/S = 0 represents the fines generated in the absence of water under the same conditions (250 rpm for 3 and 60 min).

tions occur at the solid and liquid interface. The BA used in this study underwent the same process of quenching. Consequently, the presence of the high content of leachable contaminants in the BA-S fraction can be related to the products formed during quenching. These quenching products (rich in contaminants) agglomerated on the surface of the bigger BA particles were separated by sieving in the form of particles ≤ 125 μm, which was approximately 4% (m/m) of the initial mass of un-sieved BA. However, even after the separation of this fraction from BA, the contents of contaminants in the BA-M and BA-L fractions were found to be above the regulatory limit (Soil Quality Decree, 2013). Therefore, a two-stage washing treatment to enhance the separation of agglomerated fine particles (≤125 μm) and contaminants from these fractions of BA was applied on these fractions.

3.2. Separation of the fine fraction (≤125 μm) by washing

The washing procedure used in this study was tailored to enhance the extraction of the soluble contaminants and agglomerated fine particles. After the washing treatment, agglomerated fine particles (≤125 μm) from BA-M and BA-L fractions were separated by sieving the washing mixture. In Fig. 5 the effect of washing duration and L/S ratio of the washing medium on the separation of fine particles is shown. For both fractions, a significant difference in the separation of fines was observed between the washing time of 3 and 60 min. The content of fines increased substantially at higher washing times, which indicates that the separation is mainly dependent on the energy applied in the washing process. Furthermore, the increase of L/S ratio of the washing mixture has a positive impact on the content of fines removed from BA-M and BA-L fractions. The quantity of fines separated in absence of water under the same treatment conditions was compared with the fines generated with L/S 1. In the presence of water (L/S = 1) the yield of BA-MF and BA-LF increased by 1.5 and 6.5 times as compared to the yield of fines liberated in the absence of water, respectively. This increase in the content of fines is attributed to the dissolution of soluble phases binding fines to the surface of BA-M and BA-L fractions. However, a decrease in the content of fines was also observed when the L/S was above 2, which indicates a change in the dynamics of the washing process. At L/S 5 and 10, the content of fines decreased because on average the particles were suspended further away from each other, thus leading to a reduction in the friction and abrasion in between BA particles. L/S 3 was selected as an optimum ratio for the separation of agglomerated fines and soluble contaminants (Section 3.5.), this treatment separated an additional 6.2% (m/m) of fines from the total material.

The elemental composition of BA-FM and BA-FL separated by washing treatment with L/S 3 for 60 min is presented in Table 3. The chemical composition of these fine fractions is very similar to the BA-S fraction. The high content of the Ca in all these fractions can be attributed to calcite, a weathering product of CaO. During the incineration process CaO is produced, which reacts when in contact with water producing $Ca(OH)_2$ upon quenching. Afterwards, under atmospheric conditions calcite is formed during weathering (Meima et al., 2002; Wei et al., 2011). Furthermore, the particle size distributions (PSD) of BA-S, BA-MF and BA-ML fractions is given in Fig. 2b. These fractions are very similar in terms of their PSD. Nevertheless, the fine fractions from BA-M and BA-L were slightly coarser because of their separation after washing treatment, which can facilitate the agglomeration of fine particles.

The XRD analysis of the BA-MF fraction (Fig. 6a) shows the presence of ettringite (idealized formula: $Ca_6Al_2(SO_4)_3(OH)_{12}{\cdot}26H_2O$) at an L/S 3 after 60 min washing. Ettringite is a common cement phase and forms in the presence of reactive $[Al(OH)_6]^{3-}$, SO_4^{2-} and Ca^{2+} at an pH above 10 (Hampsoim and Bailey, 1982). At longer

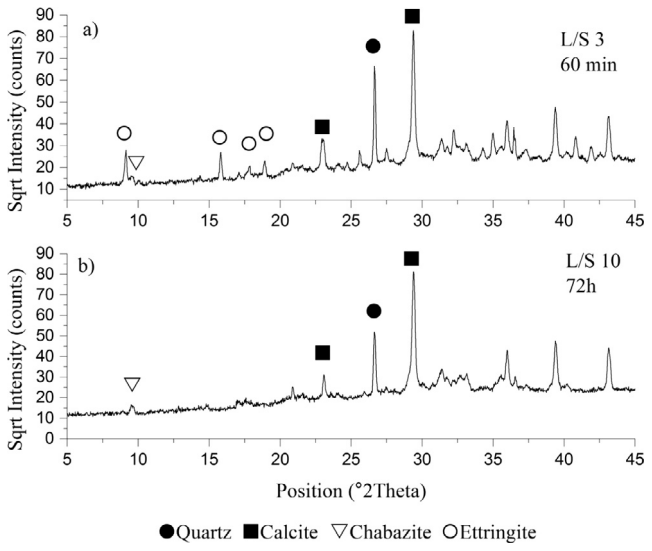

Fig. 6. XRD diffractogram of BA-MF fraction separated under different washing conditions. (a) Ettringite peak from BA-MF fraction separated after washing with L/S 3 for 60 min, and (b) BA-MF fraction separated with washing treatment at L/S 10 for 72 h showing absence of ettringite peak.

Table 3
Elemental composition (% m/m) of the fine fractions (BA-MF, BA-LF) separated by washing at L/S 3 for 60 min and initial BA-S fraction determined with XRF.

	Mg	Al	Si	P	S	K	Ca	Ti	Cr	Mn	Fe	Cu	Zn	Sr	Ba	Pb	Cl	LOI
BA-MF	0.9	6.7	5.8	0.8	2.6	1.0	41.8	1.9	0.1	0.3	7.5	0.7	1.7	0.2	0.3	0.4	0.2	27.1
BA-LF	1.1	7.1	6.9	0.9	2.7	1.1	40.7	1.9	0.1	0.3	8.3	0.6	1.7	0.2	0.3	0.3	0.3	25.5
BA-S	1.1	7.7	7.9	1.0	2.7	1.3	34.4	1.6	0.1	0.3	8.5	0.6	1.5	0.1	0.2	0.2	2.1	27.5

washing times, the dissolution of ettringite is likely to follow according to Eq. (1) (Section 3.3). Consequently, the presence of ettringite is not visible in the BA-MF fraction (Fig. 6b) separated with washing treatment of 72 h (L/S 10). A similar trend was observed for the BA-LF fraction (Fig. A.1, Appendix A). In the dissolution of ettringite, the washing duration plays a more dominant role than the L/S ratio, as discussed in Section 3.3.

3.3. Leaching of chlorides and sulfates from BA fractions

The leaching behavior of chlorides under the influence of different washing conditions such as time and L/S ratio is illustrated in Fig. 7. The amount of chlorides leached from the BA-M and BA-L fractions during the washing treatment (L/S 10) of 3 min, 6 min and 72 h remains fairly constant. A similar trend in the leaching of chlorides during washing treatment of 3 and 60 min was noted at all studied L/S ratios. Consequently, it can be concluded that the leaching of chlorides is an availability-controlled process (Sabbas et al., 2003) and a washing duration longer than 3 min does not lead to any significant increase in the removal of chlorides. In contrast to washing time, L/S ratio have a substantial effect on the leachability of chlorides. The leaching of chlorides was accelerated with the higher L/S ratios. A significant increase in the extraction of chlorides of 73% for the BA-M and 67% for BA-L fraction was observed by increasing the L/S from 1 to 2 (washing duration 60 min). However, above L/S 2, a steady increase in the leaching of chlorides was observed for both fractions. This peculiar leaching behavior of chlorides from incineration residues is widely reported in literature (Abbas et al., 2003; Kim et al., 2005; Yang et al., 2012).

The SEM image for an un-sieved bottom ash (≤4 mm), showing the morphology of particles, distribution of chlorine and sulfur is provided in Fig. 8. The BA particles were found to be covered in a layer (Fig. 8a), the formation of which is discussed in Section 3.1. Moreover, it is also evident from the elemental mapping that the majority of the chlorine (Fig. 8b) and sulfur (Fig. 8c) were distributed on the surface of particles. Contrary to it, the internal structure of majority of BA particles was empty in term of these elements. However, in some BA particles, chlorine was found to be distributed homogenously throughout the whole particle (bottom right of Fig. 8b). Nevertheless, the extraction of similar contents of chlorides irrespective of washing time (Fig. 7) suggests that the majority of chlorides are attached to the particle surface, thus facilitating their rapid leaching upon contact with water.

In spite of numerous studies focusing on the removal of chlorides from BA, there is a lack of information regarding their speciation. The speciation of the chlorides in BA residues is a challenging task due to the complex chemistry of material. Consequently, the presence of chlorides in BA is less understood. The leaching behavior of the most commonly occurring cations (Na^+, K^+ and Ca^{2+}) with respect to chlorides under the influence of different L/S ratios at

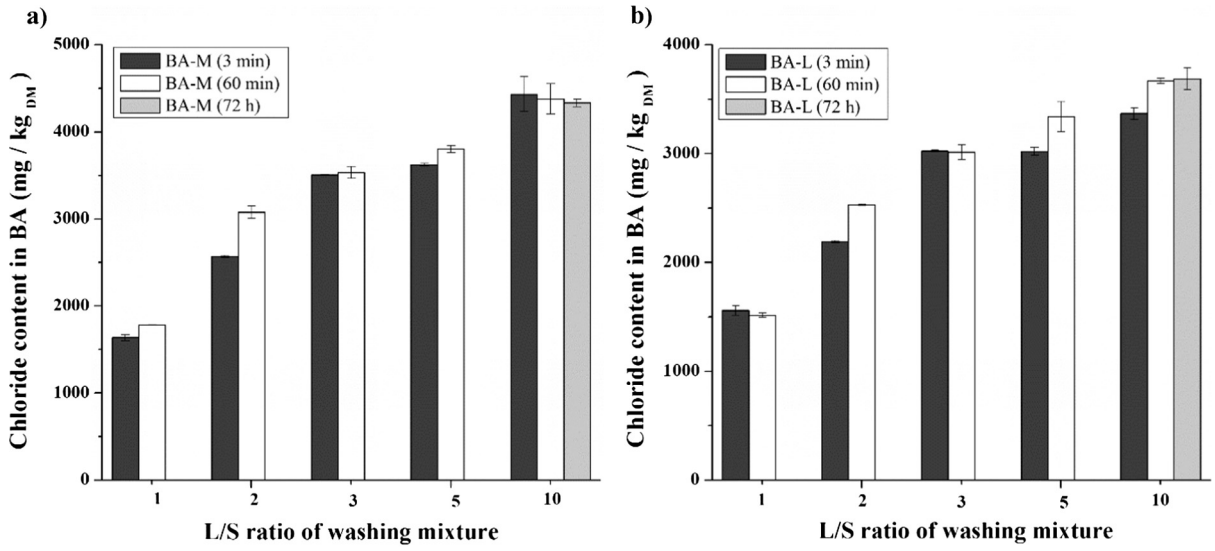

Fig. 7. Soluble content of chloride in BA fractions (a) BA-M (0.125–1 mm) and (b) BA-L (1–4 mm) under the influence of washing time of 3, 60 min and 72 h at different L/S ratios.

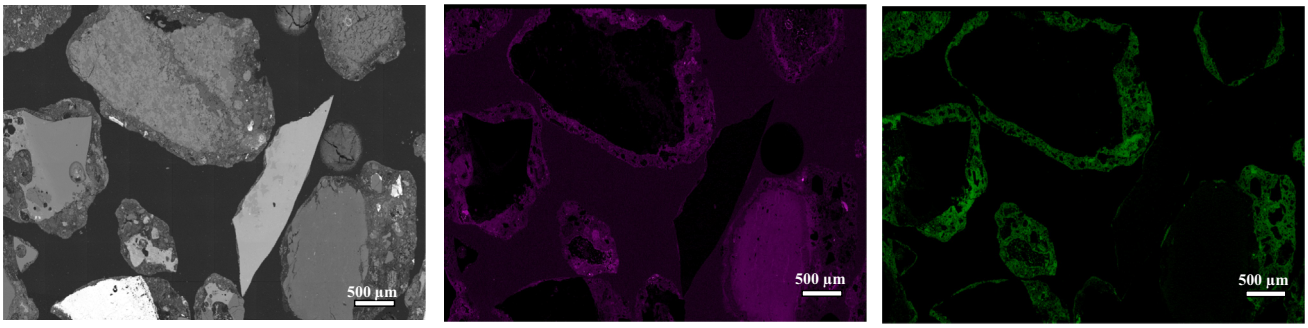

a) b) c)

Fig. 8. Cross-section of un-sieved bottom ash (≤4 mm) and its elemental mapping (a) BSE-SEM image (b) Chlorine and (c) Sulfur.

60 min is presented in Fig. 9. The concentration of these ions increased with the increase of water used for the washing treatment. The release rate of Na^+ from BA matrix to the leachates closely followed the leaching rate of chlorides, in a molar ratio of 1:1. This strong correlation in the leaching behavior and molar ratio of these ions suggests the presence of NaCl in bottom ash residues. On the other hand, the dissolution rates of K^+ and Ca^{2+} do not show a significant increase at higher L/S and their amount in leachates is considerably lower compared to chlorides (solubility of NaCl and KCl, 358 and 254 g/kg at 20 °C, respectively). A similar leaching behavior of Na^+, K^+, Ca^{2+} and chlorides was found in the leachates generated by washing BA-L fraction under the same conditions (Fig. A.2, Appendix A). It can be concluded that NaCl is one of the soluble chloride salts in BA residues. However, from the solubility point of view of pure NaCl, a washing treatment with L/S 1 should be sufficient to achieve complete dissolution before reaching saturation limit. Likewise, the leaching trend of Na^+ and Cl^- observed in washing experiments with different L/S ratios is also different from the solubility behavior of pure sodium chloride. It can be argued that the retention of washing water in the BA due to its high porosity (Bendz et al., 2007) limits the release of the chlorides. At lower L/S ratios, the washing water is more concentrated with chlorides, thus its sorption will lead to the retention of a higher amount of chlorides in the bottom ash. Therefore, an increase in the L/S ratio will produce a less concentrated solution of chlorides, ultimately adsorbing less chlorides in the BA matrix. Furthermore, highly complex chemistry of BA material, porosity, water retention along with a presence of other chemical species plays an important role in influencing the dissolution of NaCl. The factors governing this behavior of chlorides in BA still remains uninvestigated.

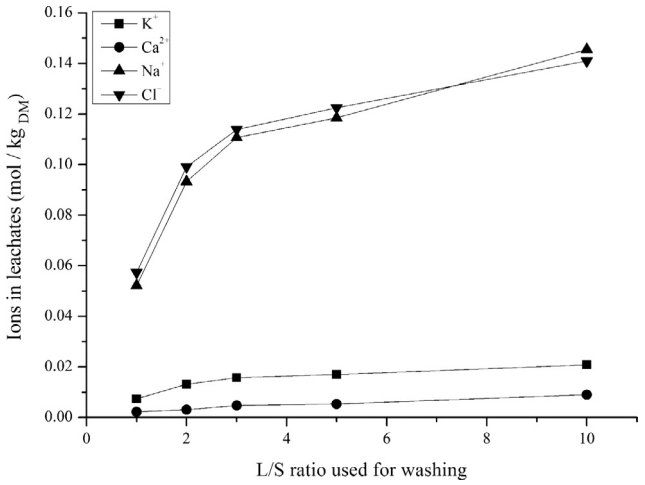

Fig. 9. Number of moles of K^+, Ca^{2+}, Na^+ and Cl^- released in leachates by the BA-M fraction (0.125–1 mm) during washing treatment by varying L/S ratio at 60 min.

After chlorides, the most abundant contaminant present in BA is sulfate. The effect of L/S ratio and washing duration of washing treatment on the leaching of sulfates is presented in Fig. 10. The leaching of sulfates from the BA-M and BA-L fractions increases gradually with the increase in L/S ratio. This increase indicates that the leaching of sulfates is a solubility-controlled phenomenon depending on the solubility of sulfate-containing phases such as ettringite and gypsum. Although all the sulfates are initially attached to the surface of BA particles as shown in Fig. 8c, their leaching is limited by the poor solubility of sulfate containing phases. The solubility product (pK_{sp}) for some known sulfate-containing phases such as ettringite (Damidot and Glasser, 1993) and gypsum (Cornelis et al., 2012) is provided by:

$$3CaO \cdot Al_2O_3 \cdot 3CaSO_4 \cdot 32H_2O \rightleftharpoons 6Ca^{2+} + 2Al(OH)_4^- + 3SO_4^{2-} + 4OH^- + 26H_2O; \quad pK_{sp} = 55.45 \tag{1}$$

$$CaSO_4 \cdot H_2O \rightleftharpoons Ca^{2+} + SO_4^{2-} + 2H_2O; \quad pK_{sp} = -4.58 \tag{2}$$

The solubility of these phases increases with the increase in L/S ratio. Therefore, the leaching of sulfates from BA is closely related to the dissolution/precipitation of sulfate containing phases.

On the other hand, longer washing times have a significant effect on the leaching of sulfates (Fig. 10). In the initial stage of washing, the formation of ettringite takes place due to the reaction of metallic aluminum in an alkaline medium and therefore successfully immobilizing a part of the soluble sulfates. However, at longer washing times, the dissolution of ettringite is favored, which consequently leads to an increase in the leaching of sulfates. In the case of both fractions, a substantial increase in the sulfate content was observed with a washing treatment of 72 h at L/S 10, whereas the leaching of sulfates at shorter washing times of 3 and 60 min does not show considerable variations. It can be concluded that the washing duration is the dominating factor with

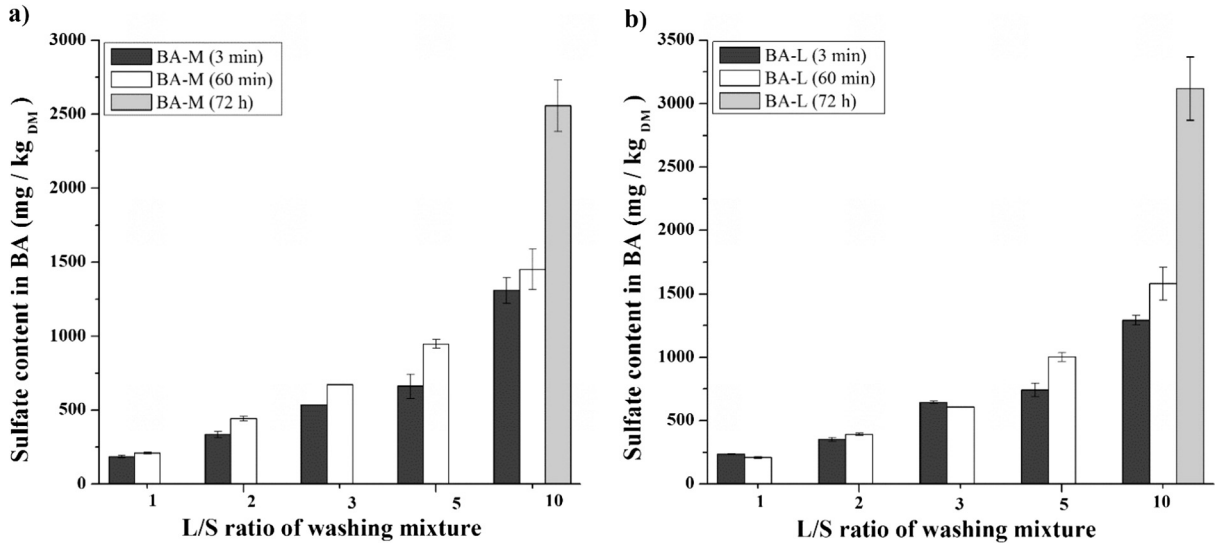

Fig. 10. Effect of washing duration and L/S ratio on the leaching of sulfates from (a) BA-M (0.125–1 mm) and (b) BA-L (1–4 mm) of MSWI bottom ash.

respect to sulfates leaching compared to L/S ratio, which is in accordance with the reported leaching behavior of sulfates from MSWI fly ash (Wang et al., 2016).

3.4. Leaching of PTEs from BA fractions

In this study, the leaching of PTEs was studied at the intrinsic pH of BA by varying the L/S ratios of the washing mixture. In the original and size-separated fractions of BA, the content of Cr, Cu, Mo and Sb exceeded their regulatory limit given in Table 2 (Soil Quality Decree, 2013). The amounts of Cr, Mo and Sb leached from the BA-M and BA-L fractions by washing for 60 min with different L/S ratios are given in Fig. 11. It is important to note that the leachates generated from both fractions of BA retain their pH value in the range of 10.9–11, irrespective of the initial amount of water. In the case of freshly produced BA, pH > 12 is due to the presence of $Ca(OH)_2$, which starts to decrease (pH range of 10–10.5) due to the formation of calcite, gypsum, gibbsite and ettringite (Chimenos et al., 2000). Furthermore, the release of PTEs (Cr, Mo and Sb) from BA enhanced with the increase in L/S ratio of mixture, which indicates that the leaching of these metals is governed by solubility-controlled phenomena. The dissolution of phases containing PTEs is favored when the amount of washing water is increased, thus leading to the increase in their leaching. The leaching of oxyanions, Cr, Mo and Sb is assumed to be controlled by the dissolution of Ca-containing minerals (Cornelis et al., 2008). In addition to the substitution of sulfates in the ettringite crystal structure by oxyanions of Cr and Mo during co-precipitation, their leaching at higher pH is also related to the solubility of $CaMoO_4$ and $BaCrO_4$, respectively (Van Gerven et al., 2005). In the case of Sb, the leaching mechanism in alkaline matrices is considered to be controlled by the solubility of romeites and the immobilization via adsorption of antimonates on the surface of ettringite (Van Caneghem et al., 2016).

In Fig. 12, a comparison between the leachable content of calcium, sulfates, Cr, Mo and Sb from the BA-L fraction after a washing treatment of 60 min is given. The similar trend in the leaching of these contaminants was observed with the increase in L/S. The increase in the content of Ca and sulfates at higher L/S can be attributed to the enhanced dissolution of their minerals, such as ettringite. Consequently, it leads to the increase in the release of Cr, Mo and Sb immobilized due to these phases. However, a high content of sulfate as compared to calcium indicates that ettringite is not the only phase contributing to the leaching of sulfates and

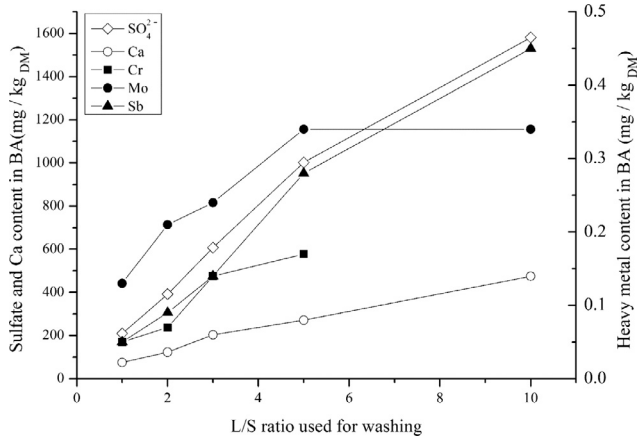

Fig. 12. The content of Cr, Mo, Sb and sulfates leached from BA-L (1–4 mm) fraction under varying L/S ratio with washing treatment of 60 min (the content of Cr at L/S 10 was under the detection limit of 20 μg/l).

subsequently to the leaching of Cr, Mo and Sb. It is also possible that the leaching of these metals is affected by the saturation of solution in term of calcium ions. However, on the basis of the correlation between the leaching of Ca, SO_4^{2-}, Cr, Mo and Sb, it can be speculated that the calcium- and sulfate-containing phases play a role in immobilizing the oxyanions of these metals. Furthermore, a similar leaching behavior of these contaminants was observed in the other fraction of BA (Fig. A.3, Appendix A).

On the other hand, in the case of Cu leaching, no systematic trend was noted at different L/S ratios. It is widely reported that the leaching of Cu is mainly related to the organic matter such as humic and fulvic acid (Arickx et al., 2010; Dijkstra et al., 2006; Olsson et al., 2007; Voglar and Leštan, 2013). Furthermore, the majority of leachable Cu in MSWI bottom ash is reported to be organically bound (Meima et al., 1999). In this study, by removing the fractions consisting of fine particles (≤125 μm), a significant content of Cu was removed. For instance, more than 70% of the total leachable Cu from the initial BA fraction was removed by separating the BA-S fraction. Moreover, high LOI (27.5% m/m) of this fraction indicates the presence of a high content of calcite and organic matter as compare to BA-M and BA-L, which in turn indicates the enrichment of organic matter and leachable Cu content in the BA-S fraction.

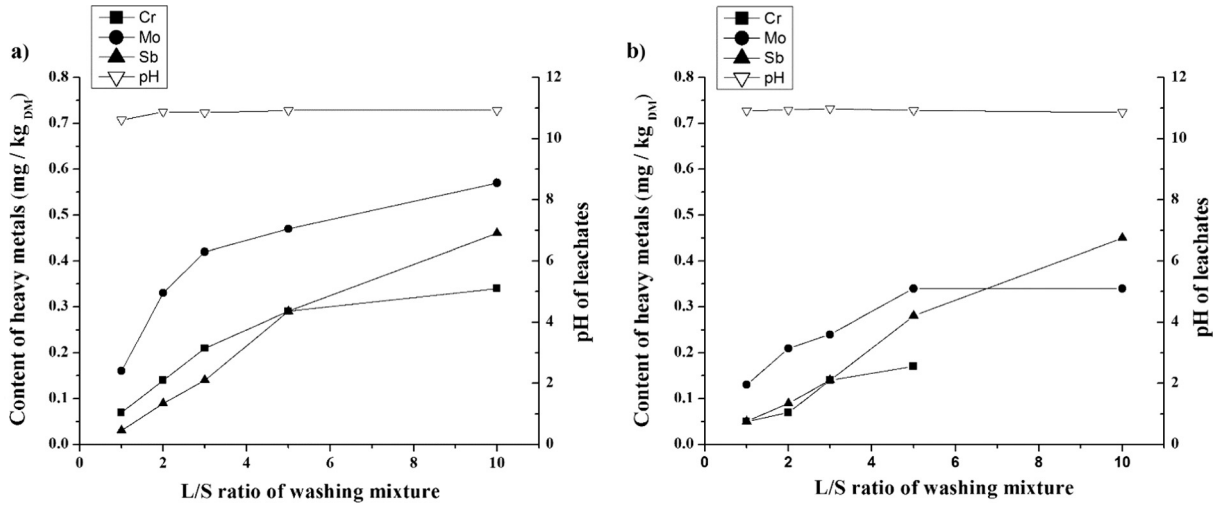

Fig. 11. Content of Cr, Mo and Sb leached during washing treatment (60 min) by increasing L/S ratio (a) BA-M (0.125–1 mm) and (b) BA-L (1–4 mm) fraction (in Fig. 11b, the amount of Cr at L/S 10 was under the detection limit of 20 μg/l).

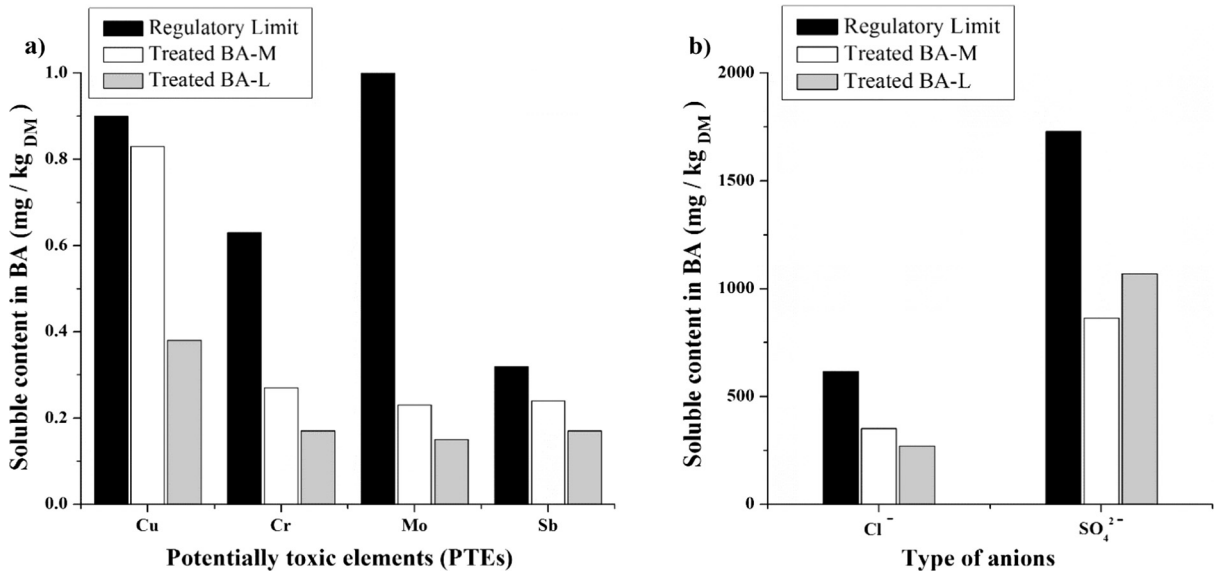

Fig. 13. Leachability of contaminants from treated BA-M (0.125–1 mm) and BA-L (1–4 mm) fractions (a) PTEs (Cu, Cr, Mo and Sb) and (b) chlorides and sulfates after applying two cycles of treatment (L/S 3, 60 min).

3.5. Optimized washing treatment

For the extraction of PTEs, chlorides and sulfates, a washing treatment with L/S 3 for 60 min was applied twice consecutively on the BA-M and BA-L fractions. The reasons for choosing two cycles of washing were: (1) The maximum amount of fine particles was separated with L/S 3 from BA-M and BA-L fractions; (2) One washing cycle with L/S 3 was not sufficient for the removal of contaminants below the legal emission limit and; (3) As discussed in Sections 3.3 and 3.4, washing with L/S higher than 3 does not show significant enhancement in the leaching of PTEs, chlorides and sulfates and using higher amounts of water is neither practical economically nor environmentally friendly. Due to these reasons, two successive washing cycles with L/S 3 were found to be effective in bringing the level of contaminants under the legal limit established by Soil Quality Decree (2013).

The leachability of PTEs, chlorides and sulfates from treated fractions of BA by applying a third washing cycle of L/S 3 (60 min) is provided in Fig. 13. The contents of Cu, Cr, Mo, Sb, Cl^- and SO_4^{2-} were reduced below the legal limit by applying this optimized washing treatment. However, the content of Cu from the BA-M fraction was slightly below the legal leaching limit after the treatment. Furthermore, a complete removal of leachable Cu by using this treatment is limited due to initial high content of Cu in the untreated bottom ash.

4. Conclusions

In this study, a two-stage treatment combining sieving and washing was applied to MSWI bottom ash (≤4 mm). This BA fraction was separated in three fractions, BA-S (≤125 μm), BA-M (0.125–1 mm), BA-L (1–4 mm) based on particle size distribution. Furthermore, washing treatment was applied for the removal of agglomerated fine particles (≤125 μm) from the BA-M and BA-L fractions.

(1) The chemical composition of all fractions containing agglomerated fine particles ≤ 125 μm, separated by both dry sieving and washing, was found to be similar. Conventional dry sieving was observed to be limited in achieving the complete removal of agglomerated fine particles. With the proposed treatment an additional 6.2% (m/m) of fines were removed from the bigger fractions of BA. The removal of these fractions from the system (≤4 mm) produces less contaminated BA which can be treated for recycling.
(2) Chlorides and sulfates, the most abundant anions in the BA, were concentrated in a layer covering the surface rather than in the interior of the particles. The presence of chlorides on the outer surface of BA particles and their high solubility results in fast dissolution irrespective of washing duration.
(3) In addition to the identification of NaCl in BA fractions by XRD, a strong correlation in the leaching mechanisms of Na^+ and Cl^- was observed, which implies that sodium chloride (NaCl) is one of the soluble salts present in MSWI bottom ash.
(4) The dissolution kinetics play an important role in the leaching of sulfates. Initially sulfate containing phases (i.e. ettringite) precipitate and subsequently dissolve again during washing. Due to this, the washing duration has a dominating influence on the leaching of sulfate compared to the L/S ratio. Therefore, at longer washing times (72 h), the leaching of sulfate increases significantly.
(5) The correlation between the leaching of Cr, Mo, Sb and SO_4^{2-} was observed, indicating that the precipitation/dissolution of the sulfate-containing phases plays a role in the mobilization of these contaminants.
(6) The clean fractions of BA were obtained by removing fine particles (≤125 μm) during dry sieving and washing treatment. The leaching of contaminants from BA-M and BA-L was brought under the Dutch legal limit by applying two consecutive washing cycles with L/S 3 for 60 min. However, their eco-toxicological impact on environment and performance in building materials need to be investigated further.

Acknowledgments

The authors would like to acknowledge the financial support provided by and STW (Stichting voor de Technische Wetenschappen), the Netherlands, under the project number 10019729: "Environmental concrete based on the treated MSWI bottom ashes". Thanks are also due to P. Tang, V. Capri and Y. Hendrix, for valuable discussions. Furthermore, the authors wish to express their grati-

tude to the following sponsors of the Building Materials research group at TU Eindhoven: Rijkswaterstaat Grote Projecten en Onderhoud; Graniet-Import Benelux; Kijlstra Betonmortel; Struyk Verwo; Attero; Enci; Rijkswaterstaat Zee en Delta-District Noord; Van Gansewinkel Minerals; BTE; V.d. Bosch Beton; Selor; GMB; Geochem Research; Icopal; BN International; Eltomation; Knauf Gips; Hess AAC Systems; Kronos; Joma; CRH Europe Sustainable Concrete Centre; Cement & Beton Centrum; Heros and Inashco (in chronological order of joining).

Appendix A. Supplementary material

Supplementary data associated with this article can be found, in the online version, at http://dx.doi.org/10.1016/j.wasman.2017.05.029.

References

Abbas, Z., Moghaddam, A.P., Steenari, B.-M., 2003. Release of salts from municipal solid waste combustion residues. Waste Manag. 23, 291–305. http://dx.doi.org/10.1016/s0956-053X(02)00154-X.

Alam, Q., Schollbach, K., Florea, M.V.A., Brouwers, H.J.H., 2016. Investigating washing treatment to minimize leaching of chlorides and heavy metals from MSWI bottom ash, in: 4th International Conference on Sustainable Solid Waste Management. Limassol, Cyprus.

Alba, N., Gasso, S., Lacorte, T., Baldasano, J.M., 1997. Characterization of municipal solid waste incineration residues from facilities with different air pollution control systems. J. Air Waste Manag. Assoc. 47, 1170–1179. http://dx.doi.org/10.1080/10473289.1997.10464059.

Arickx, S., De Borger, V., Van Gerven, T., Vandecasteele, C., 2010. Effect of carbonation on the leaching of organic carbon and of copper from MSWI bottom ash. Waste Manag. 30, 1296–1302. http://dx.doi.org/10.1016/j.wasman.2009.10.016.

Bayuseno, A.P., Schmahl, W.W., 2010. Understanding the chemical and mineralogical properties of the inorganic portion of MSWI bottom ash. Waste Manag. 30, 1509–1520. http://dx.doi.org/10.1016/j.wasman.2010.03.010.

Bendz, D., Tüchsen, P.L., Christensen, T.H., 2007. The dissolution kinetics of major elements in municipal solid waste incineration bottom ash particles. J. Contam. Hydrol. 94, 178–194. http://dx.doi.org/10.1016/j.jconhyd.2007.05.010.

Boghetich, G., Liberti, L., Notarnicola, M., Palma, M., Petruzzelli, D., 2005. Chloride extraction for quality improvement of municipal solid waste incinerator ash for the concrete industry. Waste Manag. Res. 23, 57–61. http://dx.doi.org/10.1177/0734242X05051017.

Bourtsalas, A., 2013. Review of WTE ash utilization processes under development in northwest Europe [WWW Document]. <http://www.seas.columbia.edu/earth/wtert/sofos/WTEBA.pdf> (accessed 7.8.16).

Chandler, R.T., Eighmy, T.T., Hertlen, J., Hjelmar, O., Kosson, D.S., Sawel, S.E., van der Sloot, H.A., Vehlow, J., 1997. Municipal Solid Waste Incinerator Residues - IAWG (International Ash Working Group). Elsevier.

Chimenos, J., Fernández, A., Nadal, R., Espiell, F., 2000. Short-term natural weathering of MSWI bottom ash. J. Hazard. Mater. 79, 287–299. http://dx.doi.org/10.1016/S0304-3894(00)00270-3.

Chimenos, J.M., Fernández, A.I., Cervantes, A., Miralles, L., Fernández, M.A., Espiell, F., 2005. Optimizing the APC residue washing process to minimize the release of chloride and heavy metals. Waste Manag. 25, 686–693. http://dx.doi.org/10.1016/j.wasman.2004.12.014.

Chimenos, J.M., Fernández, A.I., Miralles, L., Segarra, M., Espiell, F., 2003. Short-term natural weathering of MSWI bottom ash as a function of particle size. Waste Manag. 23, 887–895. http://dx.doi.org/10.1016/S0956-053X(03)00074-6.

Cornelis, G., Van Gerven, T., Vandecasteele, C., 2012. Antimony leaching from MSWI bottom ash: modelling of the effect of pH and carbonation. Waste Manag. 32, 278–286. http://dx.doi.org/10.1016/j.wasman.2011.09.018.

Cornelis, G., Johnson, C.A., Van Gerven, T., Vandecasteele, C., 2008. Leaching mechanisms of oxyanionic metalloid and metal species in alkaline solid wastes: a review. Appl. Geochem. 23, 955–976. http://dx.doi.org/10.1016/j.apgeochem.2008.02.001.

Damidot, D., Glasser, F.P., 1993. Thermodynamic investigation of the $CaO{\cdot}Al_2O_3{\cdot}CaSO_4{\cdot}H_2O$ system at 25 °C and the influence of Na_2O. Cem. Concr. Res. 23, 221–238. http://dx.doi.org/10.1016/0008-8846(93)90153-Z.

Dijkstra, J.J., Van Zomeren, A., Meeussen, J.C.L., Comans, R.N.J., 2006. Effect of accelerated aging of MSWI bottom ash on the leaching mechanisms of copper and molybdenum. Environ. Sci. Technol. 40, 4481–4487. http://dx.doi.org/10.1021/es052214s.

Doudart de la Grée, G.C.H., Florea, M.V.A., Keulen, A., Brouwers, H.J.H., 2016. Contaminated biomass fly ashes - characterization and treatment optimization for reuse as building materials. Waste Manag. 49, 96–109. http://dx.doi.org/10.1016/j.wasman.2015.12.023.

Dutch Ministry of Infrastructure and Environment, 2012. Greendeals GD076: Sustainable useful application of WtE bottom ash [WWW Document]. <http://www.greendeals.nl/gd076-verduurzaming-nuttige-toepassing-aec-bodemassen/> (accessed 8.9.16).

Eighmy, T.T., Eusden, J.D., Marsella, K., Hogan, J., Domingo, D., Krzanowski, J.E., Stämpfli, D., 1994. Particle petrogenesis and speciation of elements in MSWI bottom ashes. Stud. Environ. Sci. 60, 111–136. http://dx.doi.org/10.1016/S0166-1116(08)71452-3.

Eusden, J.D., Eighmy, T.T., Hockert, K., Holland, E., Marsella, K., 1999. Petrogenesis of municipal solid waste combustion bottom ash. Appl. Geochem. 14, 1073–1091. http://dx.doi.org/10.1016/S0883-2927(99)00005-0.

Florea, M.V.A., Brouwers, H.J.H., 2015. Treatment of incineration by-products for generating new building materials. In: 19th Ibausil, International Conference on Building Materials (Internationale Baustofftagung). Weimar, Germany, pp. 1505–1512.

Hampsoim, C.J., Bailey, J.E., 1982. On the structure of some precipitated calcium alumino-sulphate hydrates. J. Mater. Sci. 17, 3341–3346. http://dx.doi.org/10.1007/BF01203504.

Hjelmar, O., 1996. Disposal strategies for municipal solid waste incineration residues. J. Hazard. Mater. 47, 345–368. http://dx.doi.org/10.1016/0304-3894(95)00111-5.

Hjelmar, O., Holm, J., Crillesen, K., 2007. Utilisation of MSWI bottom ash as sub-base in road construction: first results from a large-scale test site. J. Hazard. Mater. 139, 471–480. http://dx.doi.org/10.1016/j.jhazmat.2006.02.059.

Holm, O., Simon, F.-G., 2017. Innovative treatment trains of bottom ash (BA) from municipal solid waste incineration (MSWI) in Germany. Waste Manag. 59, 229–236. http://dx.doi.org/10.1016/j.wasman.2016.09.004.

Inkaew, K., Saffarzadeh, A., Shimaoka, T., 2016. Modeling the formation of the quench product in municipal solid waste incineration (MSWI) bottom ash. Waste Manag. 52, 159–168. http://dx.doi.org/10.1016/j.wasman.2016.03.019.

Ito, R., Dodbiba, G., Fujita, T., Ahn, J.W., 2008. Removal of insoluble chloride from bottom ash for recycling. Waste Manag. 28, 1317–1323. http://dx.doi.org/10.1016/j.wasman.2007.05.015.

Juric, B., Hanzic, L., Ilić, R., Samec, N., 2006. Utilization of municipal solid waste bottom ash and recycled aggregate in concrete. Waste Manag. 26, 1436–1442. http://dx.doi.org/10.1016/j.wasman.2005.10.016.

Keulen, A., Florea, M.V.A., H.J.H., B., 2012. Upgrading MSWI bottom ash as building material for concrete mixes. In: 18th Ibausil, International Conference on Building Materials (Internationale Baustofftagung). Weimar, Germany.

Kim, S.-Y., Tanaka, N., Matsuto, T., Tojo, Y., 2005. Leaching behaviour of elements and evaluation of pre-treatment methods for municipal solid waste incinerator residues in column leaching tests. Waste Manag. Res. 23, 220–229. http://dx.doi.org/10.1177/0734242X05055322.

Margallo, M., Taddei, M.B.M., Hernández-Pellón, A., Aldaco, R., Irabien, Á., 2015. Environmental sustainability assessment of the management of municipal solid waste incineration residues: a review of the current situation. Clean Technol. Environ. Policy 17, 1333–1353. http://dx.doi.org/10.1007/s10098-015-0961-6.

Meima, J.A., van der Weijden, R.D., Eighmy, T.T., Comans, R.N., 2002. Carbonation processes in municipal solid waste incinerator bottom ash and their effect on the leaching of copper and molybdenum. Appl. Geochem. 17, 1503–1513. http://dx.doi.org/10.1016/S0883-2927(02)00015-X.

Meima, J.A., van Zomeren, A., Comans, R.N.J., 1999. Complexation of Cu with dissolved organic carbon in municipal solid waste incinerator bottom ash leachates. Environ. Sci. Technol. 33, 1424–1429. http://dx.doi.org/10.1021/es971113u.

Olsson, S., van Schaik, J.W.J., Gustafsson, J.P., Kleja, D.B., van Hees, P.A.W., 2007. Copper(II) binding to dissolved organic matter fractions in municipal solid waste incinerator bottom ash leachate. Environ. Sci. Technol. 41, 4286–4291. http://dx.doi.org/10.1021/es062954g.

Pera, J., Coutaz, L., Ambroise, J., Chababbet, M., 1997. Use of incinerator bottom ash in concrete. Cem. Concr. Res. 27, 1–5. http://dx.doi.org/10.1016/S0008-8846(96)00193-7.

Sabbas, T., Polettini, A., Pomi, R., Astrup, T., Hjelmar, O., Mostbauer, P., Cappai, G., Magel, G., Salhofer, S., Speiser, C., Heuss-Assbichler, S., Klein, R., Lechner, P., 2003. Management of municipal solid waste incineration residues. Waste Manag. 23, 61–88. http://dx.doi.org/10.1016/S0956-053X(02)00161-7.

Soil Quality Decree, 2013. Regeling Bodemkwaliteit, VROM, Den Haag: Ruimte en Milieu. Ministerie van Volkshuisvesting, Ruimtelijke Ordeling en Milieubeheer.

Speiser, C., Baumann, T., Niessner, R., 2000. Morphological and chemical characterization of calcium-hydrate phases formed in alteration processes of deposited municipal solid waste incinerator bottom ash. Environ. Sci. Technol. 34, 5030–5037. http://dx.doi.org/10.1021/es990739c.

Tang, J., Steenari, B.-M., 2015. Leaching optimization of municipal solid waste incineration ash for resource recovery: a case study of Cu, Zn, Pb and Cd. Waste Manag. 48, 315–322. http://dx.doi.org/10.1016/j.wasman.2015.10.003.

Tang, P., Florea, M.V.A., Spiesz, P., Brouwers, H.J.H., 2016. Application of thermally activated municipal solid waste incineration (MSWI) bottom ash fines as binder substitute. Cem. Concr. Compos. 70, 194–205. http://dx.doi.org/10.1016/j.cemconcomp.2016.03.015.

Tang, P., Florea, M.V.A., Spiesz, P., Brouwers, H.J.H., 2015. Characteristics and application potential of municipal solid waste incineration (MSWI) bottom ashes from two waste-to-energy plants. Constr. Build. Mater. 83, 77–94. http://dx.doi.org/10.1016/j.conbuildmat.2015.02.033.

Van Caneghem, J., Verbinnen, B., Cornelis, G., de Wijs, J., Mulder, R., Billen, P., Vandecasteele, C., 2016. Immobilization of antimony in waste-to-energy bottom ash by addition of calcium and iron containing additives. Waste Manag. 54, 162–168. http://dx.doi.org/10.1016/j.wasman.2016.05.007.

Van Gerven, T., Van Keer, E., Arickx, S., Jaspers, M., Wauters, G., Vandecasteele, C., 2005. Carbonation of MSWI-bottom ash to decrease heavy metal leaching, in view of recycling. Waste Manag. 25, 291–300. http://dx.doi.org/10.1016/j.wasman.2004.07.008.

Voglar, G.E., Leštan, D., 2013. Equilibrium leaching of toxic elements from cement stabilized soil. J. Hazard. Mater. 246, 18–25. http://dx.doi.org/10.1016/j.jhazmat.2012.11.058.

Wang, K.-S., Sun, C.-J., Yeh, C.-C., 2002. The thermotreatment of MSW incinerator fly ash for use as an aggregate: a study of the characteristics of size-fractioning. Resour. Conserv. Recycl. 35, 177–190. http://dx.doi.org/10.1016/S0921-3449(01)00121-5.

Wang, L., Chen, Q., Jamro, I.A., Li, R.D., Baloch, H.A., 2016. Accelerated co-precipitation of lead, zinc and copper by carbon dioxide bubbling in alkaline municipal solid waste incinerator (MSWI) fly ash wash water. RSC Adv. 6, 20173–20186. http://dx.doi.org/10.1039/C5RA23889G.

Wei, Y., Shimaoka, T., Saffarzadeh, A., Takahashi, F., 2011. Mineralogical characterization of municipal solid waste incineration bottom ash with an emphasis on heavy metal-bearing phases. J. Hazard. Mater. 187, 534–543. http://dx.doi.org/10.1016/j.jhazmat.2011.01.070.

Yang, R., Liao, W.-P., Wu, P.-H., 2012. Basic characteristics of leachate produced by various washing processes for MSWI ashes in Taiwan. J. Environ. Manage. 104, 67–76. http://dx.doi.org/10.1016/j.jenvman.2012.03.008.

Yang, S., Saffarzadeh, A., Shimaoka, T., Kawano, T., 2014. Existence of Cl in municipal solid waste incineration bottom ash and dechlorination effect of thermal treatment. J. Hazard. Mater. 267, 214–220. http://dx.doi.org/10.1016/j.jhazmat.2013.12.045.